Catalysis Today xxx (2014) xxx–xxx

Contents lists available at ScienceDirect

Catalysis Today

journal homepage: www.elsevier.com/locate/cattod

Crystalline and narrow band gap semiconductor $BaZrO_3$: Bi–Si synthesized by microwave–hydrothermal synthesis

R. Borja-Urby[a,b,*], L.A. Diaz-Torres[b], I. Garcia-Martinez[a], D. Bahena-Uribe[a], Gilberto Casillas[a], A. Ponce[a], M. Jose-Yacaman[a]

[a] Department of Physics and Astronomy, The University of Texas at San Antonio, One UTSA Circle, San Antonio, TX 78249, United States
[b] Grupo de Espectroscopia de Materiales Avanzados y Nanoestructurados (GEMANA), Centro de Investigaciones en Óptica, A.C., Loma del Bosque 115, Lomas del Campestre, C.P. 37150 León, Gto., México

ARTICLE INFO

Article history:
Received 14 November 2013
Received in revised form 30 May 2014
Accepted 7 July 2014
Available online xxx

Keywords:
Photocatalyst
Nanomaterial
$BaZrO_3$
Microwave synthesis

ABSTRACT

Necessity-oriented materials design has become a priority for every nation conscious of the well-being of the environment. A suitable environmentally friendly microwave-hydrothermal reaction was used to synthesize $BaZrO_3$. A study of the properties of pure Si doped, and Bi–Si co-doped $BaZrO_3$ semiconductors is presented. Crystalline structure, morphology and optical properties were dependent on the concentration of bismuth. Well faceted and spherical particles with increasing sizes from 90 up to 500 nm were obtained as the bismuth concentration increased. The highly crystalline compounds produced, maintain the $BaZrO_3$ cubic perovskite phase even at bismuth–silicon concentrations as high as 50 and 1.5 mol%, respectively. The optical absorption edge shifts into the visible-light region and the band gap narrows as the bismuth concentration increases. Suitable compounds were obtained at reaction times of 1 and 4 h at 170 °C in water–ethanol solvent for non-doped $BaZrO_3$ and doped $BaZrO_3$, respectively. Since similar properties of other semiconductor materials have practical application as visible light-active photocatalysts, we propose the potential use of nanocomposite $BaZrO_3$ as a green photocatalyst. The effects of bismuth–silicon inclusions on the properties of $BaZrO_3$ and its relation with photocatalytic properties are exposed. HREM, HAADF and dopant distributions inside the perovskite structure are presented.

1. Introduction

Water and air pollution are two of many environmental problems that industrialized nations need to solve. In recent decades, photocatalysis by semiconductor materials has been a very active research field with respect to environmental issues such as water and air remediation. With scientific and technological development, new applications for known semiconductor materials are sought for photocatalysis, which is a vital field in the chemical industry.

After Fujishima and Honda's breakthrough ultraviolet light-induced water cleavage experiments, solar energy conversion by semiconductor materials like TiO_2 has been used for water splitting, as well as to eliminate microorganism and hazardous waste in water via photocatalysis [1,2]. Even though TiO_2 is the most reliable semiconductor for use as a photocatalyst activated by UV-light, its intrinsic band gap makes pure TiO_2 an inefficient material to be use as a visible light-active photocatalyst.

Efficient use of renewable energy sources such as sunlight, demands alternative materials capable of using light from the visible region of the electromagnetic spectrum. In 2008, Yuan et al. conducted studies on the splitting of water into O_2 and H_2 by irradiating $BaZrO_3$ with UV-light for the first time. Later, the same group confirmed improvements to this procedure using $BaZrO_3$:Sn^{4+} without the aid of a co-catalyst. They concluded that water splitting was possible due to the cubic phase of $BaZrO_3$, its disperse conduction band, and the greater electronegativity of Sn^{4+} than that of Zr^{4+} [3,4].

It is known that by changing the material composition, the electronic band structure is modified. In some cases, this has the effect of extending the optical absorption response into the visible region of the electromagnetic spectrum [5,6]. In addition, such compositional changes should enhance the materials structural stability, which is essential in order to withstand the photocatalytic processes without phase transformation.

Wang et al. tested the structural stability of Ti doped β-Bi_2O_3 under visible light irradiation. They found that the titanium functioned as a structural stabilizer of β-Bi_2O_3 during the photocatalytic

* Corresponding author at: Centro de Nanociencias y Micro y Nanotecnologías (CNMN), Instituto Politécnico Nacional (IPN), 07738 México D.F., Mexico. Tel.: +52 55 5729 6000x57526.
E-mail addresses: rborjau@ipn.mx, borjaurby.raul@gmail.com (R. Borja-Urby).

http://dx.doi.org/10.1016/j.cattod.2014.07.010
0920-5861/

decomposition of organic dyes under visible light irradiation [7]. Oxidative photocatalysts with ABO_3 structures have proven to be great chemical stabilizers in the past. Tang et al. used $CaBi_2O_4$ to decompose acetaldehyde and methylene blue. They proved that after the photocatalytic degradation of the organic contaminants, the crystalline structure of $CaBi_2O_4$ remained unchanged [8]. Enhancement of photocatalytic activity of bismuth based materials is due to the disperse nature of the s orbital of bismuth, which allows high mobility for the photocharge carriers, and to the hybridization of O 2p and Bi 6s in the valance band which narrows the band gap [9].

Physical properties of synthesized materials depend on their crystalline and electronic structures, both of which are tailored during the reaction. Recently, Dong et al. synthesized hollow $BaZrO_3$ nanospheres with both green photoluminescence and adsorption properties by adjusting the base concentration and reaction temperature during the hydrothermal process [10]. Intensive study of $BaZrO_3$ by Moreira et al. related these photoluminescence emissions to local disorder and loss of symmetry in the octahedral ZrO_6 and dodecahedral BaO_{12} constituent polyhedrons of $BaZrO_3$ [11]. Even though conventional hydrothermal process has proved to be a facile methodology to obtain pure and highly crystalline $BaZrO_3$ with particle sizes of nanometric scale, after bismuth doping at a 10 mol% concentration, second phase segregation of monoclinic ZrO_2 was detectable.

However, after the substitution of bismuth into the cubic perovskite $BaZrO_3$ structure, its optical absorption properties shifted to the visible light region. This allowed the compound to be activated by visible sunlight and to decompose methylene blue [12]. Implementing microwave irradiation to assist the synthesis of different materials, like glass and ceramic, has reduced considerably the reaction time and temperature of conventional synthesis protocols because of the dielectric heating and polarization effects of this type of irradiation. Improvements in the control of reaction parameters such as temperature, pressure and the capability to stir the precursors suspended in solvent solution, rendered materials with better morphology, size and dispersability [13–15].

In the present work, the microwave–hydrothermal (M–H) method was used to synthesize Bi doped $BaZrO_3$ compounds at concentrations of 10, 30 and 50 mol%, and Bi–Si co-doped $BaZrO_3$ compounds by adding silicon at a fixed concentration of 1.5 mol%. By increasing the reaction time and temperature, it was possible to synthesize Bi doped $BaZrO_3$ and Bi–Si co-doped $BaZrO_3$ without second phase segregation up to 30 mol% Bi and 10 mol% Bi-–1.5 mol% Si, respectively, whilst preserving the $BaZrO_3$ cubic perovskite phase and particles in the nanometer size range with a narrow energy band gap. Transmission electron microscopy was used to confirm particle sizes, as well as the sphere-like morphology of the synthesized compounds. Finally, elemental analysis by energy dispersive X-ray spectroscopy (EDS) showed the constitutive elements of the $BaZrO_3$ nanoparticles, and high resolution electron microscopy images confirmed the cubic phase of $BaZrO_3$ in compounds doped up to 50 mol% Bi.

2. Materials and methods

All chemicals including barium nitrate (BaN_2O_6, 99%), zirconyl chloride octahydrate ($ZrOCl_2{\cdot}8H_2O$, 99%), bismuth nitrate pentahydrate ($BiN_3O_95{\cdot}H_2O$, 98%), powder silica gel (SiO_2), sodium hydroxide (NaOH, 99.9%) and decyl-trimethyl-ammonium bromide ($CTABC_{19}H_{42}BrN$, 98%) were purchased from Sigma-Aldrich and used without any further purification. Similar to a typical process [16], $BaZrO_3$ precursors were dissolved independently in deionized water and ethanol in a 1:1 ratio at 25 °C under constant stirring for 1 h. Stoichiometric amounts of barium (180 mM) and zirconium (180 mM) salts were added; 0.65 mM of CTAB was used as a dispersant agent to avoid particle adhesion and NaOH (1 M) was used as the precipitant agent.

Table 1
Samples of $BaZrO_3$ synthesizes by M–H process as a function of dopant concentration, reaction temperature, reaction time estimated optical bandgap and cell parameter.

Sample	Dopant (mol%)		Temperature (°C)	Time (min)	Band gap (eV)	Cell parameter (Å)
	Bi	Si				
1	–	–	170	60	3.15	4.2192
2	10	–	170	60	4.89	4.2201
3	10	–	170	120	4.56	4.2288
4	10	–	170	240	3.36	4.2289
5	30	–	170	240	3.15	4.2223
6	50	–	170	240	2.66	4.3309
7	–	1.5	170	240	3.74	4.2251
8	10	1.5	170	240	3.15	4.2274
9	30	1.5	170	240	2.52	4.2218
10	50	1.5	170	240	4.15	4.2953

The mixture was transferred to a 2.5 ml glass vial. Different samples of $BaZrO_3$ doped with high bismuth concentration (10 mol% Bi, 30 mol% Bi and 50 mol%Bi) and 1.5 mol% Si were synthesized at different temperatures, as listed in Table 1, in a Biotage initiator + microwave furnace under 900 rpm, 9 bar and 35 W. After the microwave–hydrothermal reaction, the slurry was separated by centrifugation, washed several times in an ultrasonic bath with ethanol to eliminate reaction residues, and dried overnight at 100 °C. Finally, the dried samples were grounded in Agata mortar for further structural, morphological and optical characterization.

3. Characterization

A series of compounds of Bi doped $BaZrO_3$ and Bi–Si co-doped $BaZrO_3$ (see Table 1) were synthesized via microwave–hydrothermal (M–H) synthesis in order to learn how the reaction parameters affect the synthesized compounds and the structural, morphological and optical properties. Crystalline phase $BaZrO_3$ samples were characterized by powder X-ray diffraction (XRD) on a Rigaku Ultima IV theta-theta type X-ray diffractomator at room temperature, with a step size of 0.02° in 2θ over the scanning angular range 10–100° at 1.54 Å. Powder $BaZrO_3$ based compounds were grounded in an Agata mortar and then dispersed in an ethanol solution, placed in a sonic bath for 5 min. UV–vis absorption spectra acquisition was then carried out in a Cary 100 UV–vis spectrophotometer from Agilent Technologies. Morphology and particle size were characterized by transmission electron microscopy (TEM) in a JEOL JEM 2010F (FEG-TEM) at 200 kV acceleration voltage. This used powder of the $BaZrO_3$ based compounds dispersed in the ethanol solution; a drop from this solution was drop casted onto a copper grid covered with carbon thin film. High angle annular dark field (HAADF) and bright field (BF) images were acquired simultaneously, and energy dispersive X-ray spectroscopy (EDS) performed in a scanning transmission electron microscope (STEM) JEOL JEM-ARM 200F with Cs corrected proof at 200 kV.

4. Results and discussion

The XRD patterns of the synthesized $BaZrO_3$ compounds listed in Table 1 are shown in Fig. 1. In each case, the obtained phase corresponded to the $BaZrO_3$ cubic crystalline phase of space group *Pm*-3*m* in accordance with the JCPDS 06-0399 standard card. Synthesis of $BaZrO_3$ compounds by the M–H process as a function of reaction parameters: time (15, 30 and 60 min) and temperature

Please cite this article in press as: R. Borja-Urby, et al., Crystalline and narrow band gap semiconductor $BaZrO_3$: Bi–Si synthesized by microwave–hydrothermal synthesis, Catal. Today (2014), http://dx.doi.org/10.1016/j.cattod.2014.07.010

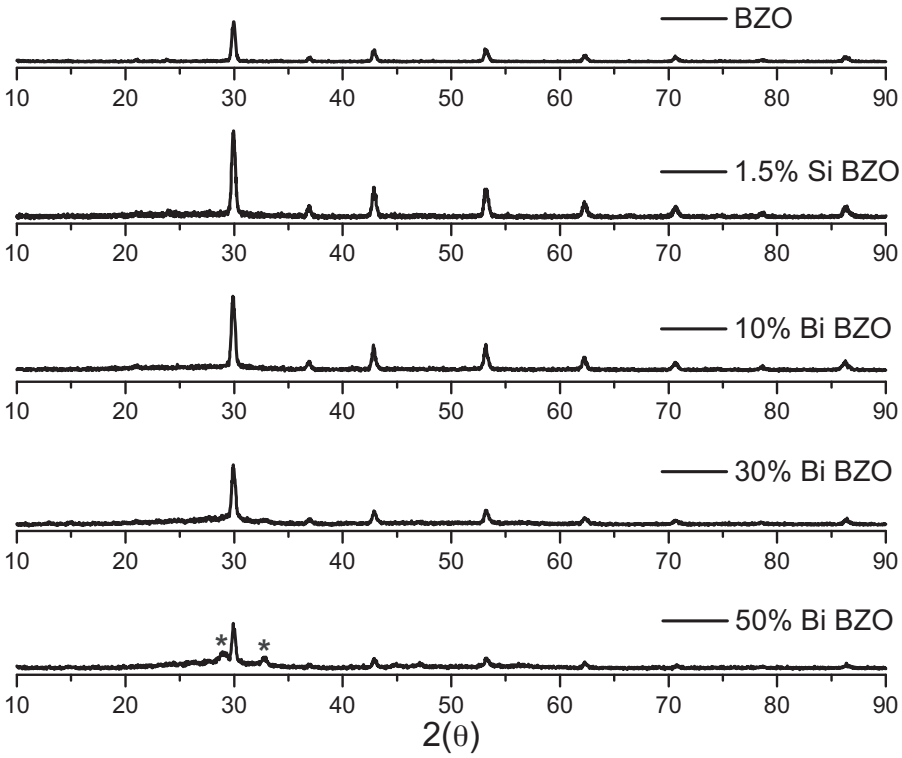

Fig. 1. X-ray diffraction pattern of non-doped $BaZrO_3$, $BaZrO_3$: 1.5 mol% Si, $BaZrO_3$: 10 mol% Bi, $BaZrO_3$: 30 mol% Bi, $BaZrO_3$: 50 mol% Bi (from top to button) indexed to JCPDS 06-0399. (*)Tetragonal phase $Bi_2O_{2.33}$ segregation in the 50 mol% Bi compound was indexed to JCPDS 27-0051.

(120, 150 and 170 °C), showed enhancement of the $BaZrO_3$ cubic crystalline phase as time and temperature increased up to 60 min and 170 °C, respectively.

Under these reaction parameters, single phase, highly crystalline $BaZrO_3$ was obtained (Fig. 1) with lattice constant $a = 4.2192$ Å which is close to reported values [17]. Moreira et al., reported that single phase and crystalline properties were favored as the M–H reaction time increased from 40 to 160 min as $BaCO_3$ segregation was almost eliminated for the larger reaction time (<0.6%) [11]. Although the $BaZrO_3$ cubic phase was indexed on samples synthesized at shorter reaction times (15 and 30 min) and lower reaction temperatures (120 and 150 °C), a secondary phase was present in these compounds, which corresponded to the main diffraction reflection of $BaCO_3$ (JCPDS 5-0378).

With regards to the 1.5 mol% Si doped $BaZrO_3$, cubic crystalline $BaZrO_3$ was obtained without second phase segregation by increasing the reaction time to 240 min (see Fig. 1). $BaZrO_3$: 10 mol% Bi samples synthesized as a function of reaction time (60, 120, 240 min) at 170 °C also confirmed a cubic crystalline phase without any second phase segregation. Introduction of bismuth ions at this molar concentration in $BaZrO_3$ compounds without second phase segregation is an improvement from our previous works on Bi doped $BaZrO_3$ by conventional hydrothermal route [12]. In said work, segregation of the ZrO_2 monoclinic phase of up to 30.9% was found in the sample with a bismuth concentration of 10 mol% Bi [12]. In that article, the visible light-active photocatalytic properties of bismuth doped $BaZrO_3$ systems was reported, achieving an 87% degradation of a solution of methylene blue under solar light irradiation despite the ZrO_2 phase segregation.

In an effort to increase further the substitution of bismuth ions into the $BaZrO_3$ crystalline structure, the compounds $BaZrO_3$: 30 mol% and $BaZrO_3$: 50 mol% were synthesized via the M–H process. It was found that bismuth ion inclusion into the $BaZrO_3$ crystalline lattice formed solid solution even at bismuth concentration as high as 50 mol% (Fig. 1). However, a slight second phase segregation of the $BaZrO_3$: 50 mol% Bi compound was indexed to the $Bi_2O_{2.33}$ tetragonal phase (JCPDS 27-0051). Thus, by the M–H synthesis process, Bi doped $BaZrO_3$ compounds can be synthesized efficiently without second phase segregation up to 30 mol% of bismuth ions. It is only at higher dosages (50 mol%) that a small amount of bismuth ions cannot be substituted into the $BaZrO_3$ crystalline structure under the present reaction parameters, which leads to a slight $Bi_2O_{2.33}$ phase segregation. This is not the case for the bismuth–silicon co-doped $BaZrO_3$ samples, as silicon ions have a detrimental effect in the $BaZrO_3$:Bi system, affecting the substitution of bismuth ions into the $BaZrO_3$ crystalline phase. This can be seen in Fig. 2, where an addition of 1.5 mol% Si ions induced segregation of tetragonal $Bi_2O_{2.33}$ in samples with 30 and 50 mol% bismuth concentrations.

In addition to the properties of conventional hydrothermal process, where the reaction takes place in a closed system under constant pressure, microwave aided processes permit a rapid increase of the solution temperature due to direct dielectric heating of the solvents, as well enhancing collisions between neighboring ions oscillating in response to the applied electromagnetic field [14,18]. By this means, reaction temperatures can be reached within seconds uniformly across the whole volume, which cannot be done by conventional hydrothermal processes. This allows the higher bismuth concentrations inclusion into the crystalline $BaZrO_3$ to form solid solution and delaying second phase segregation until concentrations as high as 50 mol% Bi are reached.

Morphological studies of pure $BaZrO_3$ samples synthesized for 1 h as a function of reaction temperature (120, 150 and 170 °C) are not shown here. TEM image analysis revealed a particle size reduction from 900 to 330 nm to 170 nm as the reaction temperature was increased up to 170 °C. In addition to bigger secondary particles, primary particles segregation was more abundant in samples synthesized at 120 and 150 °C. Well faceted particles as small as 60 nm were observed with a reaction temperature of 170 °C. The same trend was found for pure $BaZrO_3$ samples synthesized as a

Please cite this article in press as: R. Borja-Urby, et al., Crystalline and narrow band gap semiconductor $BaZrO_3$: Bi–Si synthesized by microwave–hydrothermal synthesis, Catal. Today (2014), http://dx.doi.org/10.1016/j.cattod.2014.07.010

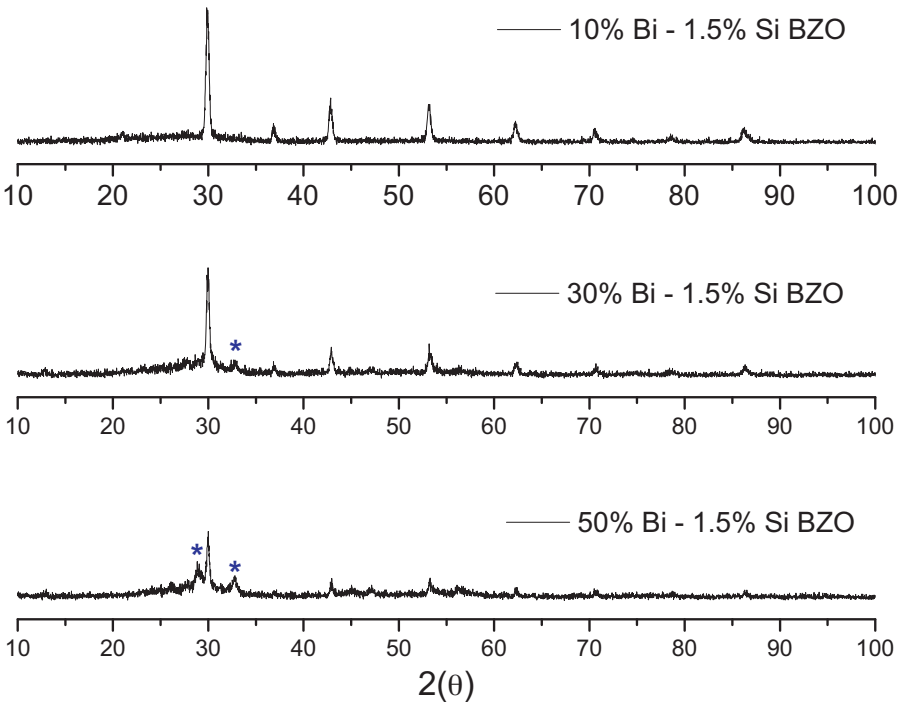

Fig. 2. X-ray diffraction pattern of Bi–Si co-doped $BaZrO_3$ compounds indexed to $BaZrO_3$ cubic phase (JCPDS 06-0399). (*) Tetragonal phase $Bi_2O_{2.33}$ segregation in the 30 and 50 mol% Bi compounds indexed to JCPDS 27-0051.

function of reaction times: 15, 30 and 60 min at a fix temperature of 170 °C; a reduction of particle size and less material segregation was observed as the reaction time increased up to 60 min. It is well known that shape and size of $BaZrO_3$ particles can be manipulated by controlling the reaction conditions [19].

Post-reaction treatments such as annealing also aid the reduction of segregation material and better quality $BaZrO_3$ particles, as demonstrated by Zhou et al. [19]. Morphology of $BaZrO_3$: 10 mol% Bi synthesized at 170 °C for 1, 2 and 4 h is shown in Fig. 3(a)–(c), respectively. Particle sizes are observed to shrink from 480 to 110 nm (±40 nm) as the reaction time increases, along with reduction of material segregation. Size reduction of pseudo-spherical microcrystalline $BaZrO_3$ was demonstrated by Lu et al., after ethanol was used as a co-solvent with water 50–50% [20]. Regarding the synthesis of $BaZrO_3$–$BaTaO_2N$, particle size reduction was observed as the Zr/Ta ratio was increased from 0 to 0.5 [21]. TEM images in Fig. 3(a)–(c) confirm that increasing both reaction time and reaction temperature favors the production of well disperse, sphere-like particles of $BaZrO_3$: 10 mol% Bi compounds as small as 100 nm.

Production of faceted and well dispersed $BaTiO_3$ nanoparticles synthesized via the M–H process were obtained by Komarneni *et al.* [15]. They reported $BaTiO_3$ products of the M–H process under stirring conditions to be smaller in size and to have better dispersibility than products prepared under static conditions. Photocatalytic studies of $BiFeO_3$ compounds conducted by Huo *et al.*, proved enhanced photocatalytic activity under visible light irradiation (>420 nm) due to well dispersed sphere-like $BiFeO_3$ particles with large surface areas and a narrow band gap (2.1 eV) [22]. TEM images of $BaZrO_3$: 30 mol% Bi and $BaZrO_3$: 50 mol% Bi displayed in Fig. 3(e) and (f), depict particle growth from 180 to 450 nm with bismuth concentration, respectively. Sphere-like

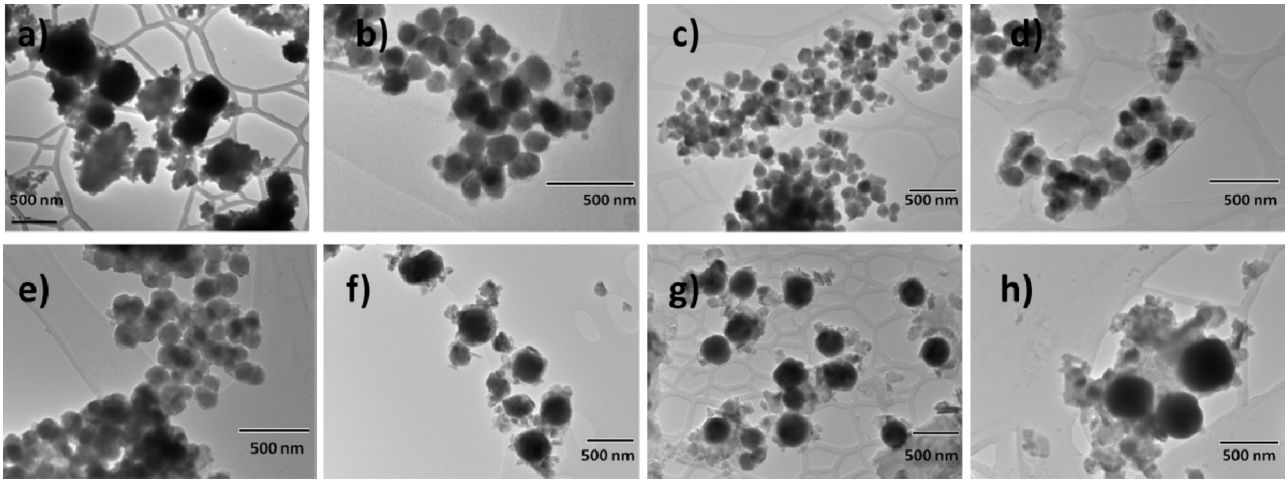

Fig. 3. TEM images of $BaZrO_3$: 10 mol% Bi synthesized at 170 °C for: (a) 1 h, (b) 2 h and (c) 4 h. Compounds synthesized for 4 h at 170 °C: (d) $BaZrO_3$: 1.5 mol% Si, (e) $BaZrO_3$: 30 mol% Bi, (f) $BaZrO_3$: 50 mol% Bi, (g) $BaZrO_3$: 30 mol% Bi–1.5 mol% Si, (h) $BaZrO_3$: 50 mol% Bi–1.5 mol% Si.

Please cite this article in press as: R. Borja-Urby, et al., Crystalline and narrow band gap semiconductor $BaZrO_3$: Bi–Si synthesized by microwave–hydrothermal synthesis, Catal. Today (2014), http://dx.doi.org/10.1016/j.cattod.2014.07.010

particles were also confirmed and material segregation appeared only at the higher concentration of 50 mol% in good agreement with the XRD data. This is consistent with an enlargement of the cell parameter (a) of doped samples as shown in Table 1 due to the larger ionic radii of bismuth (103 pm) compared to zirconium (72 pm). In regard to the $BaZrO_3$: 1.5 mol% Si compound, particle sizes in the range of 110 ± 40 nm with little material segregation was observed in the TEM images (see Fig. 3d). Similar to single doped $BaZrO_3$:Bi compounds, silicon co-doped $BaZrO_3$: 30 mol% Bi and $BaZrO_3$: 50 mol% Bi compounds synthesized under the same reaction parameters (Fig. 3(g) and (h)) followed the same trends; a particle size increment from 150 to 450 nm as the bismuth concentration was increased. In addition, a more severe material segregation was observed starting at 30 mol% Bi in co-doped samples.

UV–vis absorption spectra of the non-doped $BaZrO_3$, $BaZrO_3$: 1.5 mol% Si and $BaZrO_3$: X mol% Bi (X = 10, 30 and 50) samples were measured in the range from 230 to 900 nm at room temperature; the information was normalized as shown in Fig. 4. Here the typical optical absorption band of $BaZrO_3$ centered at 255 nm can be seen [3]. Broadening of the absorption band can be related to some extend to unintentional silicon contamination from the glass vial used in the synthesis method, as some Na and Si ions can be exchanged during the reaction. Despites this, it is still possible to observe the absorption edge red shifted into the visible range, which is more notorious on the $BaZrO_3$: 50 mol% Bi sample.

It is well known that the optical absorption edge of semiconductor compounds can be extended into the visible region by inducing vacancies to the lattice of the compounds [9]. This trend was observed by Khan *et al.*, upon the substitution of tantalum (Ta) into $BaZrO_3$. They found that the absorption edge red shifted as the Ta concentration was increased to 4% [6]. Optical properties of semiconductor materials are defined by the gap between the

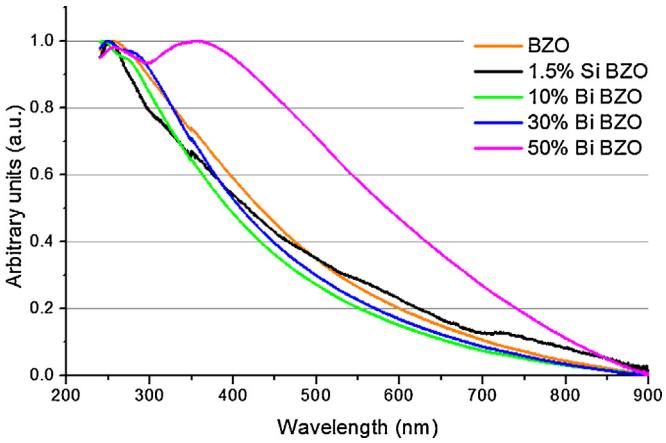

Fig. 4. UV–vis absorption spectra of undoped and doped $BaZrO_3$ compounds.

valance and conduction bands. Electrons which are trapped and localized in this gap strongly interact with the lattice structure, and modify the optical properties of the compounds. In order to estimate the optical band gap energy (E_g) of each sample, the information from their respective absorption spectra was converted into Munk–Kubelka units, based on the relation $(\alpha h\nu)^2 = k(h\nu - E_g)$, where $h\nu$ is the energy of the incident light in eV, k a constant, and α is the absorption coefficient. In Fig. 5, E_g was estimated by extrapolating the linear portion of the Tauc plots. The E_g of synthesized, non-doped $BaZrO_3$ sample is rather narrow (E_g = 3.15 eV). Cavalcante *et al.*, estimated via ab initio calculations that oxygen vacancies due to Zr–O bond break induce local structural disorder which narrows the E_g of $BaZrO_3$ compounds [23].

After bismuth substitution, the optical band gap energy of $BaZrO_3$:Bi samples narrowed from 3.36 to 2.66 eV with increasing

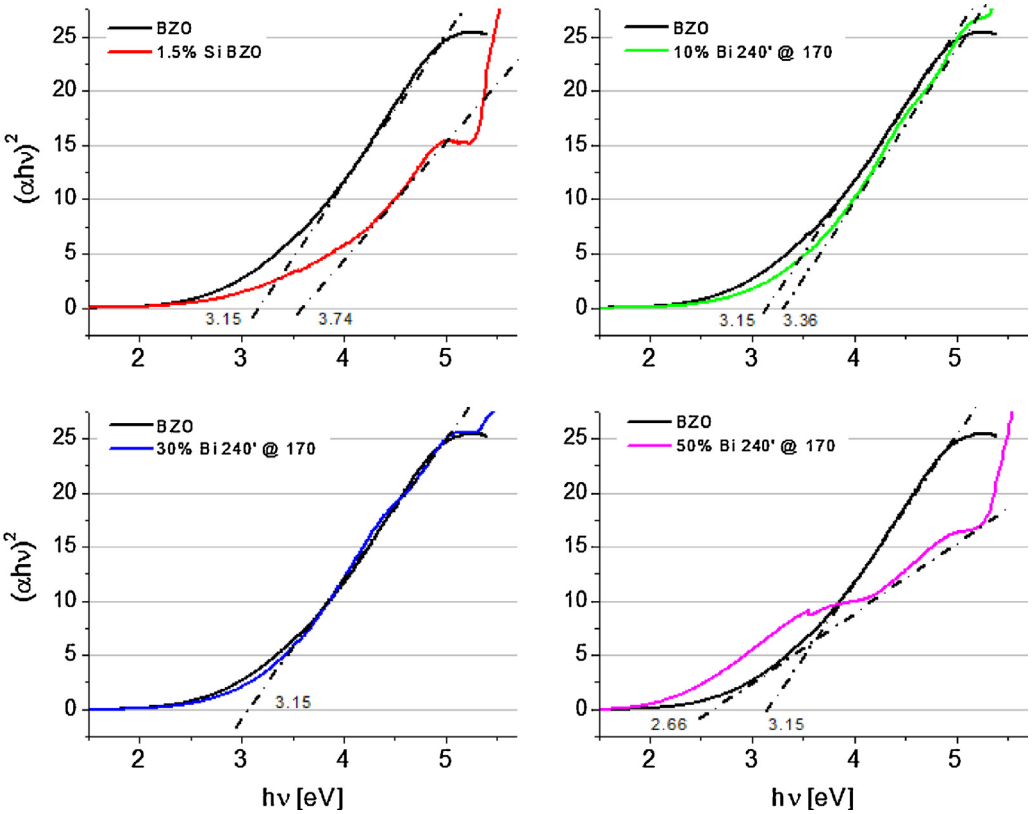

Fig. 5. Band gap estimation of non doped $BaZrO_3$ (3.15 eV) sample along with doped sample: (a) 1.5 mol% Si, (b) 10 mol% Bi, (c) 30 mol% Bi and (d) 50 mol% Bi displayed in Tauc plots after their respective UV–vis absorption spectra.

Please cite this article in press as: R. Borja-Urby, et al., Crystalline and narrow band gap semiconductor $BaZrO_3$: Bi–Si synthesized by microwave–hydrothermal synthesis, Catal. Today (2014), http://dx.doi.org/10.1016/j.cattod.2014.07.010

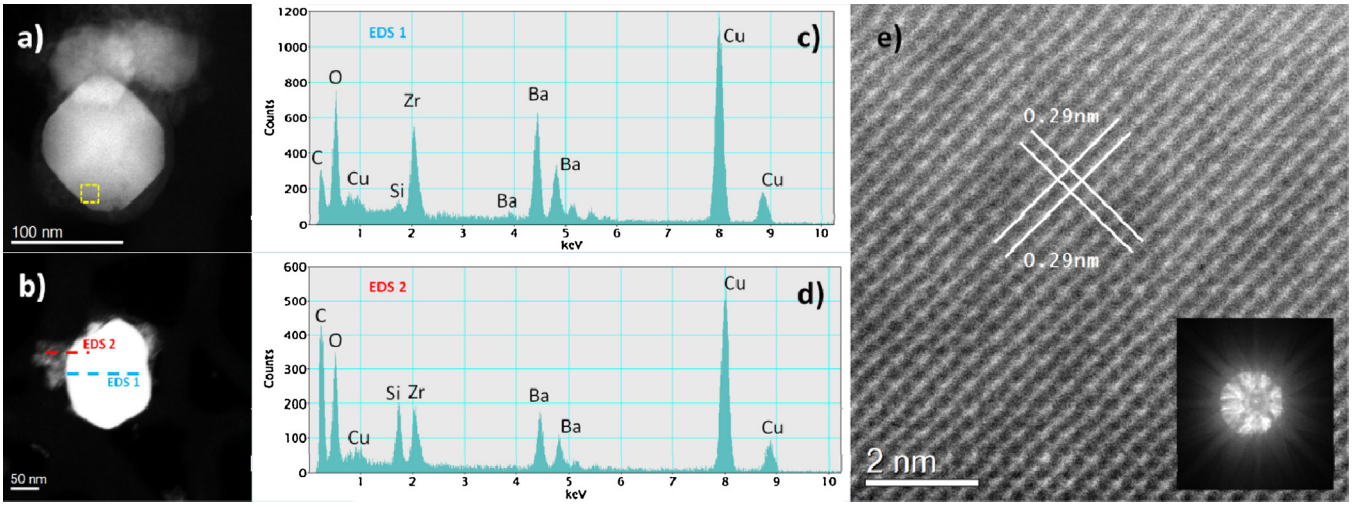

Fig. 6. Representative HAADF image of $BaZrO_3$ nanoparticle (a) line scans on nanoparticle and on material segregated (b) EDS 1 on nanoparticle shown in (b). (c) EDS 2 on both material segregated and nanoparticle shown in (b). (d) HREM image of square section marked in (a), the inset shows the Kickuchi lines corresponding to zone axis [0 0 1] (e).

bismuth concentration, which confirms the observed red shift of the absorption edge. In part this can be related to a greater density of trapped electrons in localized states due to increasing distortions of the local structure after bismuth substitution [24]. Moreover, after bismuth is substituted into the $BaZrO_3$ structure, the valance band spreads due to hybridization of Bi 6s and O 2p orbitals, thus narrowing the gap between valance and conduction bands [8]. Further insight on the electronic structure of these materials can be obtained through the photoluminescence spectra reported in previous work [2].

Electron microscopy high angle annular dark field (HAADF) techniques are capable of differentiating the constitutive elements within a compound as a function of the atomic number (Z), since the image contrast depends on Z^n (the value of n is close to 2) [25]. Observation of the spatial distribution of Er ions in ZrO_2 by means of HAADF-STEM imaging and theoretical simulation has helped in the understanding of the photoluminescent properties of ZrO_2:Er compounds [26]. Representative HAADF and high resolution electron microscopy (HREM) images of pure $BaZrO_3$ are shown in Fig. 6. Gray contrast on the HAADF image indicates uniform spatial distribution of elements on the nanoparticle. Nanoparticles and the segregated material around them were analyzed by energy-dispersive X-ray spectroscopy (EDS). It was found that the nanoparticles are mostly constituted of Ba, Zr and O atoms (see line scanning in Fig. 6(c)) with a small amount of Si contamination which increases when the line scan included the segregated material around the nanoparticle as shown in Fig. 6(d).

HREM images were obtained after correct orientation of the nanoparticle as shown by the Kicuchi lines (see inset in Fig. 6). The columns of atoms associated to the (1 1 0) cubic plane with interplanar distance of 0.29 Å appear without appreciable dislocations and confirms the $BaZrO_3$ composition of the compound.

HREM images of $BaZrO_3$: 30 mol% Bi and $BaZrO_3$: 50 mol% Bi nanoparticles in Figs. 7 and 8, respectively, depict atomic planes corresponding to the [0 0 1] zone axis without appreciable dislocations. From EDS Ba, Zr, O and Bi were found to be the main elements on the nanoparticle. The signal profiles of each element in Fig. 7(b) taken after the line scan on the inset in (a), showed that the segregated material is constituted mainly of Si contamination, which is also found in low concentration along the nanoparticle. As expected, the Bi signal in the EDS line-scan increases with concentration from $BaZrO_3$: 30 mol% Bi to $BaZrO_3$:

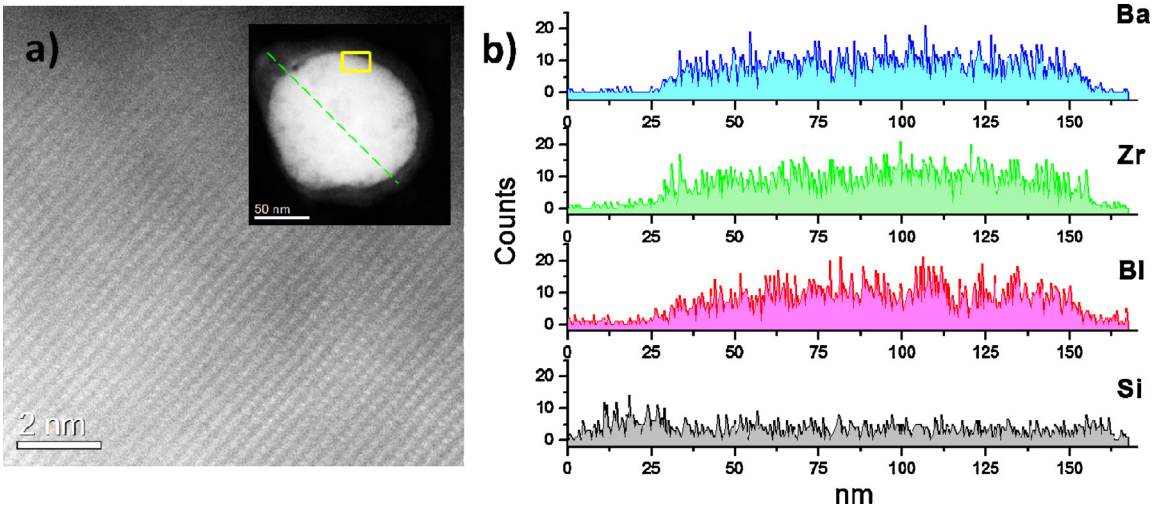

Fig. 7. (a) High resolution STEM-DF image of $BaZrO_3$: 30 mol% Bi compound, the inset shows one typical sphere-like nanoparticle with size around 125 nm, the square depicts the area where the high resolution image was taken from. (b) EDS elemental signal profile from the line scan shown in the inset on (a).

Please cite this article in press as: R. Borja-Urby, et al., Crystalline and narrow band gap semiconductor $BaZrO_3$: Bi–Si synthesized by microwave–hydrothermal synthesis, Catal. Today (2014), http://dx.doi.org/10.1016/j.cattod.2014.07.010

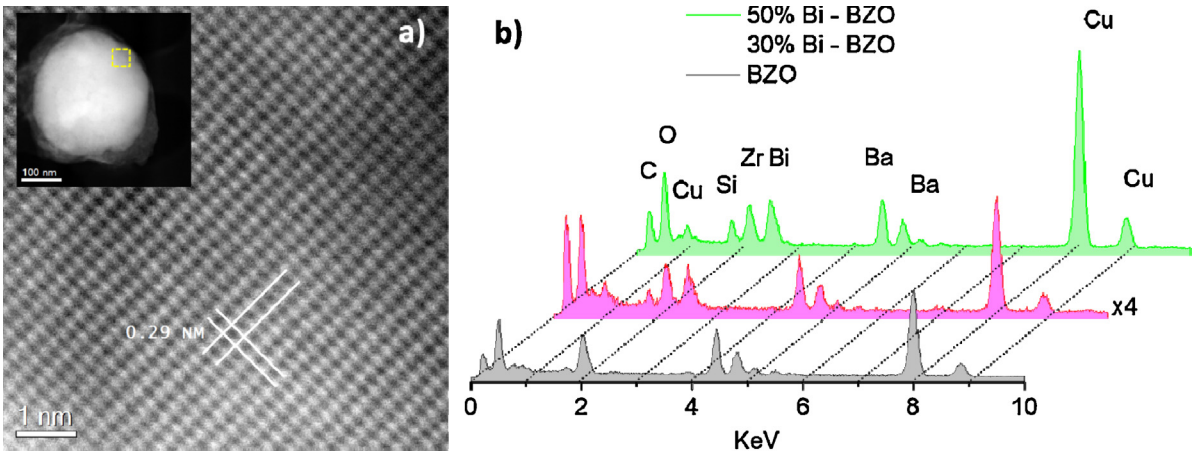

Fig. 8. (a) High resolution STEM-DF image of $BaZrO_3$: 50 mol% Bi compound on zone axis [0 0 1]. Inset shows one typical sphere-like nanoparticle with size around 315 nm. (b) EDS line-scan of non-doped $BaZrO_3$, $BaZrO_3$: 30 mol% Bi and $BaZrO_3$: 50 mol% Bi.

50 mol% Bi as shown in Fig. 8(b). Whereas crystalline nanoparticles of pure $BaZrO_3$ were easily synthesized through M–H process within 1 h of reaction, a longer reaction time was needed when high concentrations of Bi were used. After exchange of Na–Si during the M–H process, we found that the silicon remains mostly as a segregated material around the nanoparticles in both Bi doped $BaZrO_3$ and Bi–Si co-doped $BaZrO_3$ compounds. As observed in Fig. 3, silicon segregation is more abundant in co-doped compounds according to EDS analysis. It is possible that silicon added as a precursor material (1.5 mol%) in the M–H process did not react along with the other constitutive elements, Ba, Zr, and Bi, due to low reaction temperatures as silicon is a weak microwave absorber [13].

5. Conclusions

By the facile microwave-hydrothermal process, highly concentrated $BaZrO_3$:Bi and $BaZrO_3$:Bi–Si crystalline nanoparticles where synthesized for 4 h at 170 °C. Bismuth concentration was increased from 10 to 30 and 50 mol% whereas silicon was fixed at 1.5 mol% for co-doped samples. Under these reaction parameters, the products preserved the ideal $BaZrO_3$ Perovskite cubic phase. Crystalline structure and particle sizes increased with reaction time and reaction temperature. Only at the highest bismuth concentration $Bi_2O_{2.33}$ segregation was observed in Bi doped $BaZrO_3$ compounds and at 30 mol% Bi–1.5 mol% Si on co-doped $BaZrO_3$ samples.

The optical band gap energy of $BaZrO_3$ compounds was reduced from 3.15 to 2.66 eV after bismuth inclusion, which locates the excitation energy of $BaZrO_3$: 50 mol% Bi composite in the visible region of the electromagnetic spectrum. Sphere-like nanoparticles with sizes in the range between 70 and 150 nm were obtained for 10 mol% Bi samples. The nanoparticle size increased with bismuth concentration, reaching sizes in the range 290–450 nm for 50 mol% Bi samples. EDS analyses confirmed that the material segregated around $BaZrO_3$ nanoparticles was Si, and that Ba, Zr, and Bi are the main elements on the nanoparticles.

In addition, we observed more material segregated on Bi–Si co-doped samples. Thus, a compromise between nanoparticle size and bismuth concentration has to be done, since higher doses of bismuth ions increase the size of the nanoparticles and red-shift the excitation energy of $BaZrO_3$:Bi compounds into the visible region. Here we reported on the microwave–hydrothermal synthesis parameters to obtain $BaZrO_3$:Bi compounds of single phase, with well dispersed sphere-like nanoparticles suitable for visible-light active photocatalytic applications.

Acknowledgments

R. Borja-Urby acknowledges Centro de Investigaciones en Optica A.C. and the Astronomy and Physics Department at the University of Texas at San Antonio for posdoctoral sponsorship.

References

[1] M.R. Hoffmann, S.T. Martin, W. Choi, D.W. Bahnemann, Chem. Rev. 95 (1995) 69.
[2] A. Fujishima, K. Honda, Nature 238 (1972) 37.
[3] Y. Yuan, X. Zhang, L. Liu, X. Jiang, J. Lv, Z. Li, Z. Zou, Int. Hydrogen Energy 33 (2008) 5941.
[4] Y. Yuan, Z. Zhao, J. Zheng, M. Yang, L. Qiu, Z. Li, Z. Zou, J. Mater. Chem. 20 (2010) 6722.
[5] J. Shi, L. Guo, Prog. Natural Sci. Mater. Int. 22 (6) (2012) 592.
[6] Z. Khan, M. Qureshi, Catal. Commun. 28 (2012) 82.
[7] Y. Wang, Y. Wen, H. Ding, Y. Shan, J. Mater. Sci. 45 (2010) 1385.
[8] J. Tang, Z. Zou, J. Ye, Angew. Chem. Int. 43 (2004) 4463.
[9] J. Tang, Z. Zou, J. Ye, J. Phys. Chem. C 111 (2007) 12779.
[10] Z. Dong, T. Ye, Y. Zhao, J. Yu, F. Wang, L. Zhang, X. Wang, S. Guo, J. Mater. Chem. 21 (2011) 5978.
[11] M.L. Moreira, J. Andres, J.A. Varela, E. Longo, Cryst. Growth Des. 9 (2) (2009) 833.
[12] R. Borja-Urby, L.A. Díaz-Torresa, P. Salas, E. Moctezuma, M. Vega, C. Ángeles-Chávez, Mater. Sci. Eng. B 176 (2011) 1382.
[13] K.J. Rao, P.D. Ramesh, Bull. Mater. Sci. 18 (4) (1995) 447.
[14] K.J. Rao, B. Vaidhyanathan, M. Ganguli, P.A. Ramakrishnan, Chem. Mater. 11 (1999) 882.
[15] S. Komarneni, H. Katsuki, Ceram. Int. 36 (2010) 1165.
[16] L.A. Diaz-Torres, P. Salas, V.M. Castaño, J. Oliva, E. De la Rosa, Nanotechniques 1 (2010) 360.
[17] A. Aimable, B. Xin, N. Millot, D. Aymes, J. Solid State Chem. 181 (2008) 183.
[18] I. Bilecka, M. Niederberger, Nanoscale 2 (2010) 1358.
[19] H. Zhou, Y. Mao, S.S. Wong, J. Mater. Chem. 17 (2007) 1707.
[20] Z. Lu, Y. Tang, L. Chen, Y. Li, J. Cryst. Growth 266 (2004) 539.
[21] K. Maeda, K. Domen, J. Catal. (2013), http://dx.doi.org/10.1016/j.jcat.2012.12.003
[22] Y. Huo, Y. Jin, Y. Zhang, J. Mol. Catal. A: Chem. 331 (2010) 15.
[23] L.S. Cavalcante, J.C. Sczancoski, V.M. Longo, F.S. De Vicente, J.R. Sambrano, A.T. de Figueiredo, C.J. Dalmaschio, M.S. Li, J.A. Varela, E. Longo, Opt. Commun. 281 (2008) 3715.
[24] L.S. Cavalcante, N.C. Batista, T. Badapanda, M.G.S. Costa, M.S. Li, W. Avansi, V.R. Mastelaro, E. Longo, J.W.M. Espinosa, M.F.C. Gurgel, Mater. Sci. Semicond. Process. 16 (2013) 1035.
[25] A. Alvaro Mayoral, F.L. Deepak, R. Esparza, G. Casillas, C. Magen, E. Perez-Tijerina, M. Jose-Yacaman, Micron (2011), http://dx.doi.org/10.1016/j.micron.2011.10.020.
[26] C. Angeles-Chavez, P. Salas, T. Lopez-Luke, E. de la Rosa, Vacuum 84 (2010) 1226.

Please cite this article in press as: R. Borja-Urby, et al., Crystalline and narrow band gap semiconductor $BaZrO_3$: Bi–Si synthesized by microwave–hydrothermal synthesis, Catal. Today (2014), http://dx.doi.org/10.1016/j.cattod.2014.07.010